

Modulational instability: first step towards energy localization in nonlinear lattices

Isabelle Daumont†, Thierry Dauxois‡ and Michel Peyrard

Laboratoire de Physique, URA-CNRS 1325, Ecole Normale Supérieure de Lyon, 46 Allée d'Italie, 69364 Lyon Cédex 07, France

Received 8 August 1996

Recommended by S Aubry

Abstract. We study the modulational instability in discrete lattices and we show how the discreteness drastically modifies the stability condition. Analytical and numerical results are in very good agreement. We predict also the evolution of a linear wave in the presence of noise and we show that modulational instability is the first step towards energy localization.

PACS numbers: 6310, 0340K, 4610, 0545

1. Introduction

The dynamical behaviour of dissipative continuous media often exhibits a spectral condensation of a certain physical quantity to a specific wavenumber region resulting in the formation of an ordered structure even when starting from an initially turbulent state or one driven by a stochastic field. Examples [1] include two-dimensional incompressible fluids, two- and three-dimensional magnetohydrodynamics fluids, atmospheres of rotating planets and electrostatic potentials in inhomogeneous magnetized plasmas.

For example, two-dimensional (2D) flows have received an important impetus from increased interest [2] in the dynamics and advection properties both in nature and experimentally. The emergence and persistence of vortex structures are the result of a remarkable property of 2D flows; in contrast to their three-dimensional counterparts, these flows are characterized by the so-called inverse-energy cascade, according to which kinetic energy shows a spectral flux to the larger scales of motion.

Phenomenologically, this intriguing property, now commonly referred to as *self-organization*, results in the instability of linear waves leading to the formation of large organized coherent structures. As such continuous media are generically described by nonlinear partial differential equations, one can ask how discrete media will behave.

It was recently shown [3] that in discrete lattices the nonlinear interaction between breather-like excitations gives rise to an energy localization; the world of discrete breather-like excitations is as merciless for the weak as the real world, since a systematic tendency to favour growth of the larger excitations at the expense of the others was emphasized. The question of how the formation of localized structures occurs in such conservative systems logically arises. If the existence and the stability of localized excitations has been extensively

† Permanent address: CRTBT (CNRS), BP166, 38042 Grenoble, France.

‡ Email: tdauxois@physique.ens-lyon.fr.

studied [4, 5, 6] in the last decade, much less is known about their creation. It is certainly one of the main questions of the future for nonlinear dynamics.

The modulational instability of a linear wave was proposed [3] as the first step toward energy localization. This phenomenon was studied in various contexts: in fluid dynamics [7], where it is usually called Benjamin–Feir instability, nonlinear optics [8] and plasma physics [9]. In previous studies [10], Kivshar and Peyrard showed that the predicted stability domains in discrete lattices are drastically modified with respect to the conventional results deduced from a continuum or even a semi-discrete approximation. We want here to complete their results and look for the possible consequences for the energy localization. Namely, we will consider the effect of a small noise added on a linear wave and, finally, we will come back to the energy localization problem.

2. Modulational instability

2.1. The model

We consider the dynamics of a one-dimensional chain of atoms with unit mass, harmonically coupled to nearest neighbours and subjected to a nonlinear substrate potential

$$V(x) = \frac{\omega_0^2 x^2}{2} - \frac{\alpha x^3}{3} - \frac{\beta x^4}{4} \quad (1)$$

where ω_0 is the frequency of small-amplitude on-site vibrations, and α and β are two parameters defining the anharmonicity. Here, we will restrict ourselves to cases where α or β are null; if $\beta = 0$ we have a nonsymmetrical potential whereas the second case, $\alpha = 0$, gives a symmetrical potential.

Denoting by $u_n(t)$ the position of the n th atom, its equation of motion is

$$\ddot{u}_n = K(u_{n+1} + u_{n-1} - 2u_n) - \omega_0^2 u_n + \alpha u_n^2 + \beta u_n^3. \quad (2)$$

First, we will study the stability of linear oscillations whose frequency ω and wavenumber q are related by the linear dispersion relation $\omega^2 = \omega_0^2 + 4K \sin^2(q/2)$; the lattice spacing is chosen as unity for the sake of simplicity.

To study the effects of the nonlinearity, we will consider oscillations in the phonon band. As the system is nonlinear, we have to take into account the first harmonics and therefore the standard procedure at this step is to introduce a few functions $F_{j,n}$. For the nonsymmetrical equation, the right choice is

$$u_n(t) = F_{1,n}(t)e^{-i\omega_0 t} + F_{0,n}(t) + F_{2,n}(t)e^{-2i\omega_0 t} + c.c. \quad (3)$$

whereas in the symmetrical case it is

$$u_n(t) = F_{1,n}(t)e^{-i\omega_0 t} + F_{3,n}(t)e^{-3i\omega_0 t} + c.c. \quad (4)$$

Let us assume that the envelopes are slowly varying ($|\dot{F}_{i,n}(t)| \ll \omega_0 |F_{i,n}(t)|$) and that the lattice is very discrete ($\omega_0^2 \gg 4K$). Neglecting higher-order harmonics, we obtain in both cases a discrete nonlinear Schrödinger (NLS) equation

$$2i\omega_0 \dot{F}_{1,n} + K(F_{1,n+1} + F_{1,n-1} - 2F_{1,n}) + \gamma |F_{1,n}|^2 F_{1,n} = 0 \quad (5)$$

where $\gamma = 3\beta$ for the symmetrical potential and $\gamma = 10\alpha^2/3\omega_0^2$ for the nonsymmetrical one (note that γ is always positive).

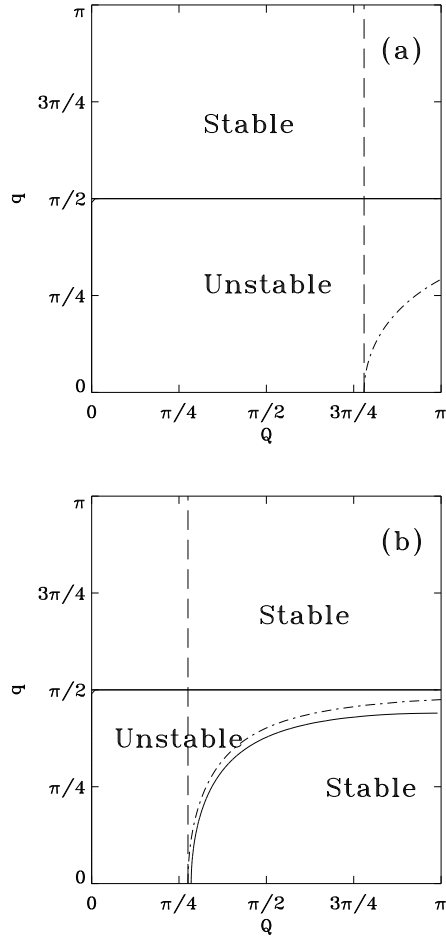


Figure 1. Stability curve. Figure (a) presents a case where $\phi_{0_c} < \phi_0$ while (b) depicts the opposite case $\phi_{0_c} > \phi_0$. The solid curve corresponds to the discrete condition (9), the dot-dashed curve to the semi-discrete and the dashed curve to the continuum limit. The words stable and unstable correspond to the discrete condition. The parameters are $\omega_0 = 10$, $K = 1$, $\beta = 1$ and $\phi_0 = 1$ for figure (a) and $\omega_0 = 10$, $K = 1$, $\beta = 0.5$ and $\phi_0 = 0.5$ for (b).

2.2. Stability conditions

The modulational instability of a plane wave in such a lattice is investigated by studying the stability of its amplitude in a function of sufficiently small perturbation so that one can linearize the equation of the envelope of the carrier wave. Therefore one introduces a small perturbation in the amplitude and in the phase, and looks for the solution

$$F_{1,n}(t) = [\phi_0 + b_n(t)]e^{i(\theta_n(t) + \psi_n(t))} \quad (6)$$

of equation (5) where $\theta_n(t) = qn - \delta\omega t$, where $2\omega_0\delta\omega = 4K \sin^2(q/2) - \gamma\phi_0^2$. Assuming $|b_n(t)| \ll \phi_0$ and $|\psi_n(t)| \ll |\theta_n(t)|$, we obtain a linear system of two equations by separating real and imaginary parts. It reads:

$$2\omega_0\dot{b}_n + K[(b_{n+1} - b_{n-1}) \sin q + \phi_0(\psi_{n+1} + \psi_{n-1} - 2\psi_n) \cos q] = 0 \quad (7)$$

$$-2\omega_0\phi_0\dot{\psi}_n + K[(b_{n+1} + b_{n-1} - 2b_n) \cos q - \phi_0(\psi_{n+1} - \psi_{n-1}) \sin q] + 2\gamma\phi_0^2 b_n = 0. \quad (8)$$

This system admits plane wave solutions with wavenumber Q and frequency Ω related by the dispersion relation

$$(\omega_0\Omega - K \sin q \sin Q)^2 = K \sin^2(Q/2) \cos q (4K \sin^2(Q/2) \cos q - 2\gamma\phi_0^2) \quad (9)$$

that we will discuss in the following paragraphs.

2.2.1. Stable wavenumbers. The perturbation b_n and ψ_n are stable only if Ω is real and therefore the condition of stability is that the right-hand side of equation (9) be positive. Because of the discreteness of the lattice, wavenumbers q and Q that differ by 2π correspond to the same wave. Thus we can restrict our study to the first Brillouin zone $[-\pi, \pi]$. Finally, we consider $[0, \pi]$ since only the direction of propagation is changing for $-q$ and $-Q$.

We note first that, in contrast to the continuum limit approximation, the stability condition depends on the wave number q : if its cosine is negative i.e. if q belongs to the interval $[\pi/2, \pi]$, the wave is stable with respect to any perturbation.

In the other case i.e., when $\cos q$ is positive, the wave is unstable when $2K \sin^2(Q/2) \cos q / \gamma \leq \phi_0^2$. Introducing a critical amplitude $\phi_{0c}^2 = 2K/\gamma$ and a critical wavenumber $q_0 = \arccos(\phi_0^2/\phi_{0c}^2)$, the wave is unstable with respect to *any* modulation provided $\phi_{0c} < \phi_0$ or $\phi_{0c} > \phi_0$ and $q > q_0$. In the case where $\phi_{0c} > \phi_0$ and $q < q_0$, only wavenumbers Q lower than $Q_{cr} = 2 \arcsin \sqrt{\phi_0^2/\phi_{0c}^2 \cos q}$ are unstable.

The results are represented in figure 1 for two different cases. We clearly see that the usual continuum limit approximation represented by the dashed line is not valid and that the modulational instability depends on the wavenumber of the carrier wave q , at least when $\phi_{0c} > \phi_0$. The figure also shows that the semidiscrete approximation [11, 12] where the carrier is treated as discrete while a continuum approximation is used for the envelope gives rather good results. However, they are wrong for example in the region with small q and high Q , where the waves are unstable in contrast to the results given by this approximation [13].

The resolution of system (8) gives not only the dispersion relation (9) but also the proportionality factor between b_0 and ψ_0 . Introducing the nondimensional number

$$\chi = \left(1 - \frac{\phi_0^2}{\phi_{0c}^2 \sin^2(Q/2) \cos q} \right)^{\frac{1}{2}}, \quad (10)$$

we obtain two different solutions for a given b_0 because of the two real frequencies ($\Omega_1 > \Omega_2$) given by equation (9):

$$u_n^1(t) = 2(\phi_0 + 2b_0 \cos(nQ - \Omega_1 t)) \cos(nq - \omega t + \frac{2\chi b_0}{\phi_0} \sin(nQ - \Omega_1 t)) \quad (11)$$

$$u_n^2(t) = 2(\phi_0 + 2b_0 \cos(nQ - \Omega_2 t)) \cos(nq - \omega t - \frac{2\chi b_0}{\phi_0} \sin(nQ - \Omega_2 t)). \quad (12)$$

We will see in the next section that both solutions should be taken into account in order to understand the behaviour of the lattice.

2.2.2. Unstable wavenumbers. If the right-hand side of equation (9) is negative, two complex conjugate numbers are solutions: the perturbation b_n diverges with the growth rate

$$\tau(Q) = |\Im m(\Omega)| = \frac{\sin(Q/2)}{\omega_0} \sqrt{2K\gamma \cos q (\phi_0^2 - \phi_{0c}^2 \sin^2(Q/2) \cos q)}. \quad (13)$$

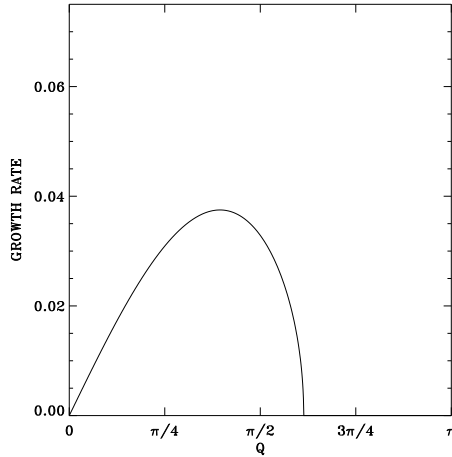


Figure 2. Growth rate versus the wavenumber of the perturbation. This case corresponds to the parameters $\omega_0 = 10$, $K = 1$, $\beta = 1$ and $\phi_0 = 1$ and $q = 5\pi/8$.

Studying this expression plotted in figure 2, we see that if $\phi_0^2 < 2 \cos q \phi_{0c}^2$ the growth rate is maximum for

$$Q_{max} = 2 \arcsin \sqrt{\frac{\phi_0^2}{2\phi_{0c}^2 \cos q}} \quad (14)$$

the perturbation corresponding to this wavenumber will play an important role. In contrast if $\phi_0^2 \geq 2 \cos q \phi_{0c}^2$, the growth rate is an increasing function of Q and the most unstable mode corresponds to $Q = \pi$.

3. Numerical verification

3.1. Numerical procedure

The results discussed in the previous section are only approximate since they are obtained not from the initial equations of motion (2) but from the nonlinear Schrödinger equation (5), derived after some hypothesis. Moreover, as we have only presented a linear stability analysis, these results deserve to be checked by numerical integrations of the equations (2) with a given initial condition. They are integrated with a fourth-order Runge–Kutta scheme with a time step chosen to conserve the energy to an accuracy better than 0.0001. Most of the simulations are performed with a chain of 256 atoms with periodic boundary conditions; this is why the wavenumbers q and Q necessarily have the forms $q = 2\pi p/N$ and $Q = 2\pi P/N$ where p and P are integers lower than $N/2$.

We chose as the initial condition a linear wave with a slightly modulated amplitude:

$$u_n(0) = (2\phi_0 + 4b_0 \cos nQ) \cos nq \quad (15)$$

$$\dot{u}_n(0) = (2\phi_0 + 4b_0 \cos nQ) \omega \sin nq \quad (16)$$

where we have neglected the frequency of the perturbation Ω in comparison with the frequency of the carrier ω . Finally, we will study the behaviour of this wave with the help

of the discrete spatial Fourier transform of the $u_n(t)$:

$$s_{p'} = \sum_{n=0}^{N-1} u_n(t) e^{\frac{2i\pi p' n}{N}}, \quad (17)$$

where p' belongs to the interval $[0, N/2]$

We will first restrict ourselves to the behaviour of the system for short times, and we will show that the results are in very good agreement with the theoretical predictions deduced from equation (9) if we take into account that the nonlinearity itself could create additional modulations. Indeed, an initial linear wave $u_n(0) = A \cos(nq)$ chosen as the initial condition will immediately create a nonlinear component $\cos^3(nq)$ if the potential (1) is symmetrical ($\alpha = 0$). As

$$u_n(0^+) = A \cos nq + d \cos^3 nq = \left[A + \frac{d}{2}(1 + \cos n2q) \right] \cos nq, \quad (18)$$

a modulation with a wavevector $Q = 2q$ is immediately generated and should be taken into account to predict the stability. These modulations have already been encountered in the analytical derivation of the NLS equation, but were later forgotten in the study of the modulational instability. However, we can derive from the expressions of the functions $F_{i,n}$ that the initial amplitude of the nonlinear perturbation is

$$d = |2F_{3,n}(0^+)| = \frac{\beta A^3}{32\omega_0^2}. \quad (19)$$

If the potential is nonsymmetrical, a modulation $Q = q$ is generated and we can similarly [14] derive its amplitude $d = |2F_{2,n}(0^+)| = \alpha A^2/6\omega_0^2$. As α and A are of the order of unity whereas $\omega_0^2 = 100$, we understand that these modulations, generated by the nonlinearity, have very small amplitudes and we can forget them unless of course they are unstable, in which case they will grow and finally play a crucial role.

3.2. Stability

Let us check numerically the stability conditions. We made different simulations plotted in figure 3 using an initial condition with $\phi_0 = 0.5$ and $b_0 = 0.0125$. We present the evolution during the first 400 time units of the amplitude of the Fourier transform of the carrier, $|s_p(t)|$, of the modulation, $|s_{2p}(t)|$, and of the third harmonic, $|s_{3p}|$, in the case of a symmetrical potential.

Figures 3(a) and 3(b) correspond to two predicted stable cases. All the parameters are identical except that the wavenumbers are chosen so that the intrinsic modulation $2q$ is stable in the first case and unstable in the second one. We clearly see that the system is stable in figure 3(a) while figure 3(b) presents the evolution of a system which becomes unstable because of the third harmonic. However, in both cases the predicted stability of the modulation is checked.

Figures 3(c) and (d) correspond to two predicted unstable cases. Figure 3(c) depicts a system where the modulation, contrary to the third harmonic, is unstable while figure 3(d) shows a case where both are unstable. As the modulation is unstable and grows exponentially, the modulation finally reaches the same order of magnitude as the carrier wave where our analytical predictions are no longer justified. We emphasize that the predictions using the discrete stability condition (9) are very accurate since in the last case the modulation wavenumber is very close to the border of the unstable region.

We have checked qualitatively the stability conditions, but we can even compute the numerical growth rate and compare it with the analytical expression (13). As attested by the

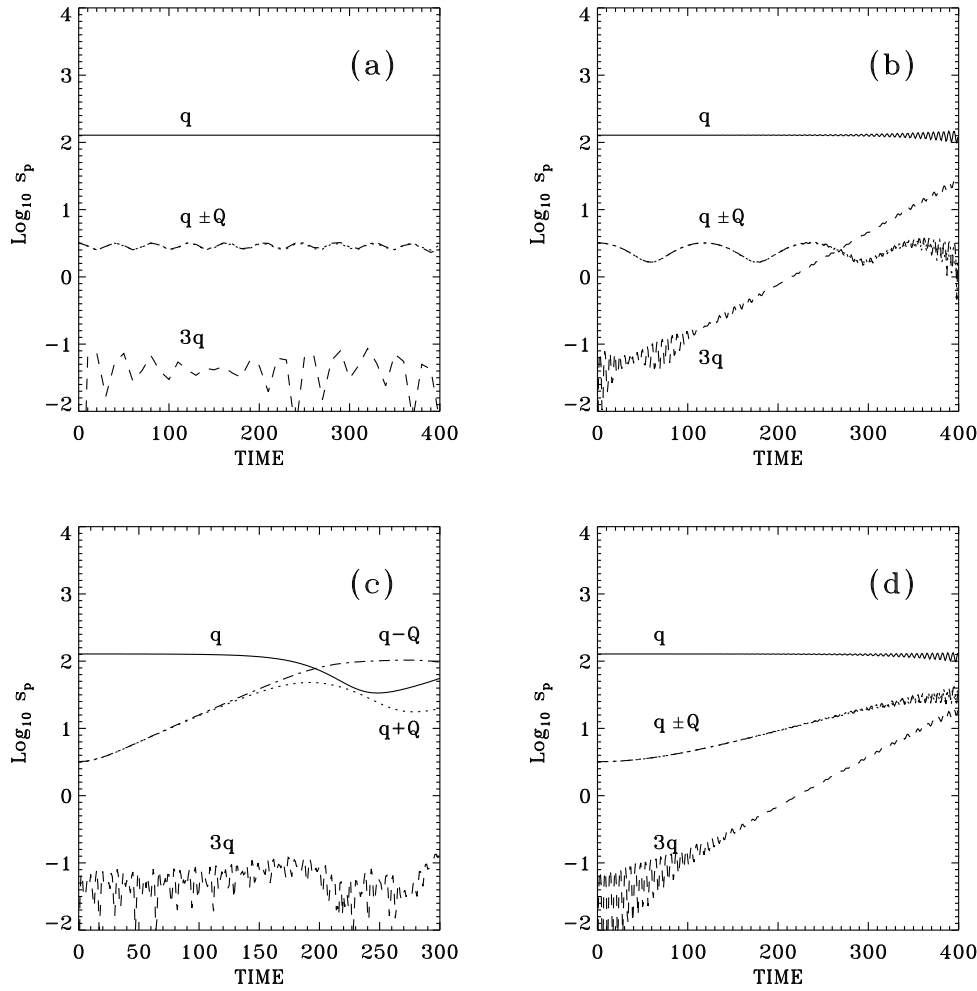


Figure 3. Evolution of the amplitude of the Fourier transform for different wavenumbers. The solid line corresponds to the initial frequency q , the dotted line to $(q + Q)$, the dash-dotted line to $(q - Q)$ and the dashed line to $3q$. The frequencies q and Q are determined from $p = 80$ and $P = 200$ for (a), $p = 30$ and $P = 80$ for (b), $p = 80$ and $P = 60$ for (c), $p = 30$ and $P = 110$ for (d). The parameters are $\beta = 0.5$, $K = 1$, $\phi_0 = 0.5$ and $\omega_0^2 = 100$. A logarithmic scale is used for the ordinate.

comparison given in table 1, the results are very accurate. However, in figures 3(a) and 3(b), we clearly see that if modulations $(q \pm Q)$ are stable their amplitudes are oscillating. The reason is that the initial condition (16) does not take into account the correction $\psi_n(t)$ on the phase and therefore does not correspond exactly to one of the two identified eigenmodes with frequency Ω_1 or Ω_2 . Consequently, this mode is decomposed over both modes and the most general initial condition is

$$u_n(0) = 2[\phi_0 \cos nq + 2(b_1 + b_2) \cos nQ] \cos\left(qn + \frac{2b_1\chi}{\phi_0} \sin nQ - \frac{2b_2\chi}{\phi_0} \sin nQ\right). \quad (20)$$

Our initial condition corresponds to $b_1 = b_2 = b_0/2$. Thus, after linearization, we obtain

$$u_n(t) = 2\phi_0 \cos(nq - \omega t) + b_0(1 + \chi) \cos[n(q + Q) - (\omega + \Omega_1)t]$$

$$\begin{aligned}
& +b_0(1 - \chi) \cos [n(q + Q) - (\omega + \Omega_2)t] \\
& +b_0(1 - \chi) \cos [n(q - Q) - (\omega - \Omega_1)t] \\
& +b_0(1 + \chi) \cos [n(q - Q) - (\omega - \Omega_2)t].
\end{aligned} \tag{21}$$

The Fourier transform then gives $|s_p(t)| = N\phi_0$ and

$$|s_{p\pm p}(t)| = Nb_0\sqrt{\cos^2(\Omega t) + \chi^2 \sin^2(\Omega t)}$$

with $\Omega = (\Omega_1 - \Omega_2)/2$. The numerical results presented in table 1 demonstrate the excellent agreement with this expression and complete the description of the system.

Table 1. *Growth rates and frequencies.* We present in this table the growth rates τ and the oscillating frequencies Ω obtained numerically (Num) and theoretically (Th). The first four lines correspond to the symmetrical potential and therefore $i = 3$; these results are obtained from figure 3. The last four lines correspond to the equivalent cases (in the same order) but for the nonsymmetrical (NS) potential ($i = 2$). S (for stable) means that there is no instability.

Figure	$\tau(q + Q)$		$\tau(iq)$		$\Omega(q \pm Q)$	
	Num	Th	Num	Th	Num	Th
3(a)	S	S	S	S	41	41
3(b)	0.018	0.018	S	S		
3(c)	S	S	0.018	0.018	115	118
3(d)	0.008	0.008	0.017	0.017		
NS-3(a)	S	S	S	S	116	114
NS-3(b)	0.003	0.004	S	S		
NS-3(c)	S	S	0.013	0.013	85	86
NS-3(d)	0.010	0.011	0.013	0.013		

3.3. Stability for long times

If the duration of a simulation is long, the evolution of an initial condition is no longer as predicted but could present two different behaviours. For a wavenumber in the interval $[0, \pi/2]$, a ‘normally’ stable wave becomes unstable because of higher harmonics, previously neglected. This phenomenon is once more a specificity of the lattices because it is due to the folding of the Brillouin zone. The nonlinearity generates modes with waves numbers $3q, 4q, 5q, \dots$, but also $2q + Q, 2q - Q, Q, \dots$. When these combinations are higher than π we have to interpret them 2π modulo. If there is an unstable region, it finally always produces unstable combinations which perturb the deduced conclusions. Figure 4 presents the prolonged simulation of figure 3(a) and we see that the stable system degenerates after 500 time units. A Fourier spectrum realized at $t = 600$ shows that some modulations are very important, particularly the frequencies $q - 3Q$ and $q + 3Q$.

In some cases, a ‘normally’ unstable modulation presents an exponentially increasing frequency until its amplitude reaches the amplitude of the carrier wave. At this stage, its amplitude decreases exponentially so that the system almost recovers its initial shape; then the increase begins again, giving rise to quasi-oscillations. Such an example is presented in figure 5. As the amplitude of the modulation becomes very important, this behaviour could not be explained by the linear stability regime and, this recurrence is reminiscent of the well-studied Fermi–Pasta–Ulam (FPU) recurrence [15] and of some other recurrences observed in continuum media [16].

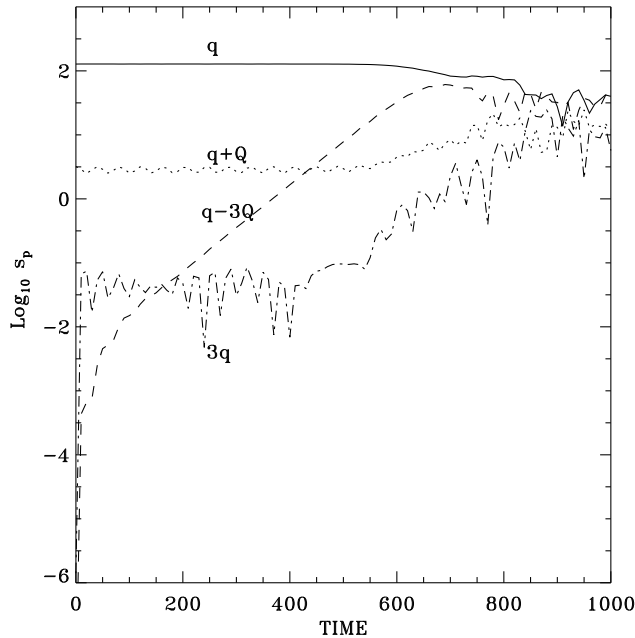


Figure 4. Same as figure 3(a) but elongated up to $t = 1000$.

However, this recurrence is different since the FPU recurrence was found in a chain of anharmonically coupled atoms which in the continuum limit gives a Korteweg–de Vries equation [17], whereas here we obtain an NLS equation. The recurrences observed in the continuum NLS equation by Yuen and Ferguson [16] are different because of the absence of the new ingredient introduced here by the discreteness through the folding of the Brillouin zone. They showed that the energy sharing process could be confined to the unstable low wavenumbers and that therefore the irreversible leakage of energy to high modes, necessary for thermalization, does not occur. Indeed, denoting the largest unstable wavenumber by q_{cr} , they showed that when $q_{cr}/2 < q < q_{cr}$, only one mode is unstable and one obtains a well-defined recurrence, whereas for $q < q_{cr}/2$, at least two modes are unstable giving rise to a so-called ‘complex evolution’.

Here, we also found that when the wavenumber is small and close to q_{cr} , the recurrence process is much longer since only very high harmonics are unstable due to the folding of the Brillouin zone. However, as has already been emphasized, any wavenumber will have an infinite number of harmonics in the unstable region (if it exists of course) and thus the recurrence will be destroyed after a finite time because of the absence of the high-wavenumber cutoff in the instability domain.

4. Noise

In the previous section, we have seen that analytical and numerical results are in very good agreement when the amplitude of a plane wave is modulated by only one wavenumber, as in equation (16). To be closer to a real situation, we will consider now the following initial condition

$$u_n(0) = (2\phi_0 + \Gamma(n)) \cos nq \quad (22)$$

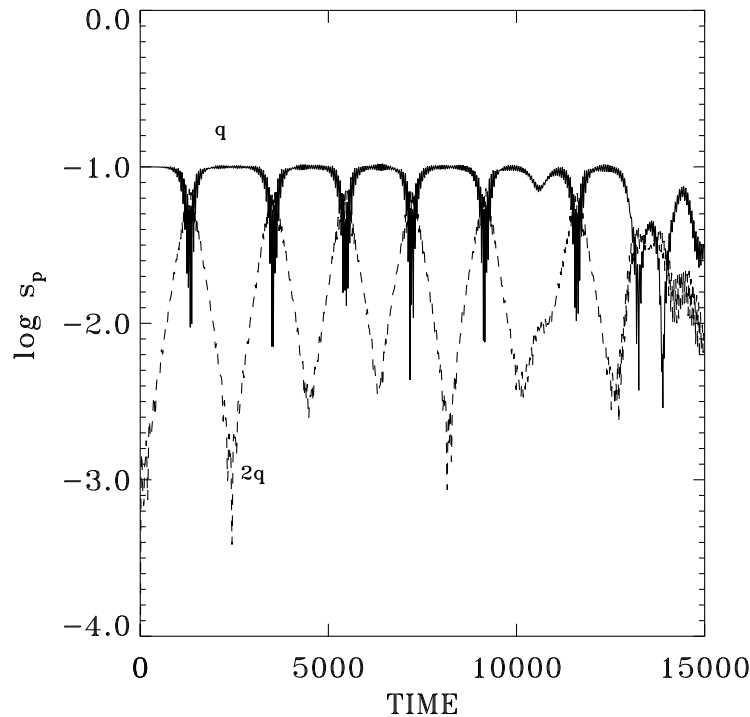


Figure 5. Recurrence. Evolution of the amplitude of the Fourier transform for wave numbers q and $2q$ versus time ($q = 0.491$). The parameters are $\alpha = 15$, $K = 1$, $\phi_0 = 0.1$ and $\omega_0^2 = 100$. A logarithmic scale is used for the ordinate.

where $\Gamma(n)$ is a gaussian noise or a white noise. Now, all frequencies have a nonzero initial amplitude and depending on their growth rates, will keep their amplitude or grow when time is increasing. In figure 6, the dotted curve corresponds to the Fourier transform of the initial condition, whereas the solid curve corresponds to the system at time $t = 150$.

All wavenumbers have approximately the same weight in the initial Fourier transform except the main frequency q whose Fourier transform amplitude corresponds to $N\phi_0/2$. In contrast, for $t = 150$, we see that two groups of frequencies, symmetric with respect to q , are unstable since their corresponding amplitudes have grown with time. Let us show that it is possible to predict not only the interval of frequencies but also the evolution of their amplitudes.

We have seen in section 2.2.1 that, if a wavenumber Q is unstable, we obtain two complex conjugate frequencies ($\Omega = \delta \pm i\tau$) where τ is the growth rate given by equation (13) and $\delta = K \sin q \sin Q/\omega_0$. Therefore one of these two modes will disappear, whereas the other one will grow exponentially. We have to stress here that we must take into account the translation of the wavenumbers. Indeed, the growth rate $\tau(Q)$, plotted in figure 2, was determined for a modulation ($\pm Q$) of a plane wave q : the wavenumber of the corresponding wave was therefore $(q \pm Q)$. If we plot the growth rate versus the wavenumber, we obtain not one but two symmetric bells, as shown in the inset of figure 6. These two symmetric intervals of unstable wavenumber explain why we clearly see on figure 6 two symmetric bells around the main frequency q .

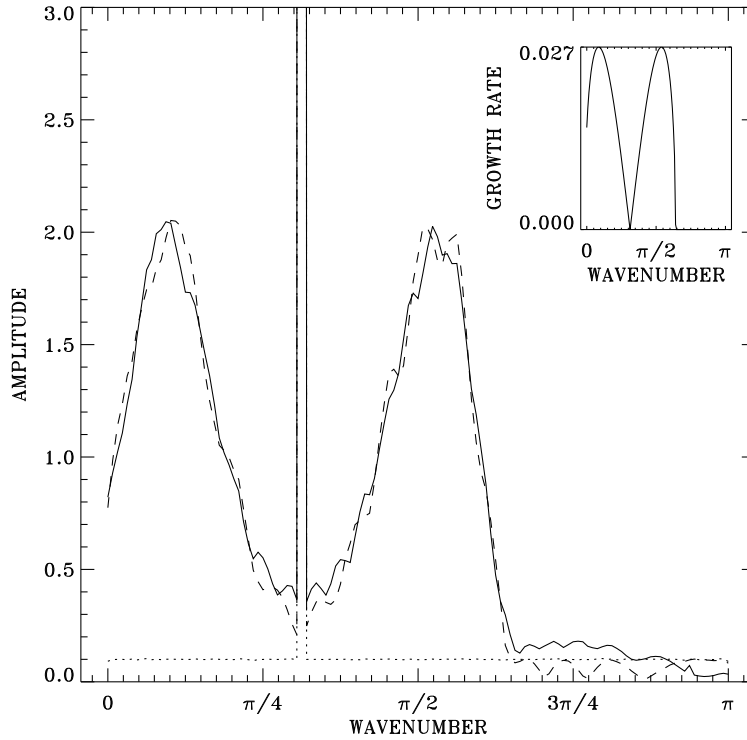


Figure 6. Noise. Amplitude of the Fourier transform of the positions versus the wavenumbers. The solid curve corresponds to the numerical results obtained at $t = 150$ by averaging 1000 simulations, the dotted curve to the initial condition and the broken curve to the analytical expression (see text). The inset presents the growth rate expression versus the wavenumber. Parameters are $\beta = 0.5$, $K = 2$, $\phi_0 = 0.6$, $\omega_0^2 = 100$ and $t_0 = 100$. The amplitude of the gaussian noise is 0.01 and its variance is 1.

To predict the growth, we have to take into account the mixing of both modes (the unstable and the vanishing): therefore the position of the n th atom is given by

$$u_n(t) = [2\phi_0 + 4b_0 \cosh(\tau t) \cos(nQ - \delta t)] \cos \left[qn - \omega t + \frac{2b_0 \chi'}{\phi_0} \sinh(\tau t) \cos(nQ - \delta t) \right]. \tag{23}$$

The Fourier transform of this expression is not as simple as in the stable case. However, given the spectrum at a given time t_0 , it is possible to predict its future evolution for a time interval $t - t_0$ by considering that each component with wavevector k evolves with its own growth rate $\tau(k)$, i.e.

$$|s_k(t)| \simeq |s_k(t_0)| e^{\tau(k) \cdot (t-t_0)}. \tag{24}$$

The above expression is very accurate as attested by the broken curve plotted in figure 6.

It is also possible to consider [14] a noise added to the plane wave and not only added to the amplitude of the cosine. This noise gives slightly different results because the added frequencies could not directly be interpreted with the above theory since the wavenumbers are not the simple modulation of a main frequency q . However, it is again possible to predict the unstable domain. Let us note that if the amplitude of the zero wavenumber is high (i.e. the case for a noise with a nonzero mean value), the harmonics will be very

important even if they are not in the unstable region. This effect is due to the nonlinearity: in section 2.2.1, we have considered a case where $F_{0,n}(0) = 0$ which gives $F_{0,n}(t) = 0$ for later times. In the presence of noise, $F_{0,n}(0) \neq 0$ and, because of the nonlinear effects, we also have $F_{2,n}(0^+) = -\beta F_{1,n}^2 F_{0,n} / \omega_0^2$. As $F_{1,n}$ is large, the harmonic will have a great value as soon as the nonlinear effects take place. The simulation results confirm these predictions.

5. Localization of energy

The previous section has addressed the study of a linear wave with a small noise when an unstable region exists; let us now consider the final evolution of this initial condition. As already emphasized, some harmonics will inevitably be in this unstable region even if the main frequency is stable. Some frequencies will therefore grow and the instability will destroy completely the coherence of the initial condition.

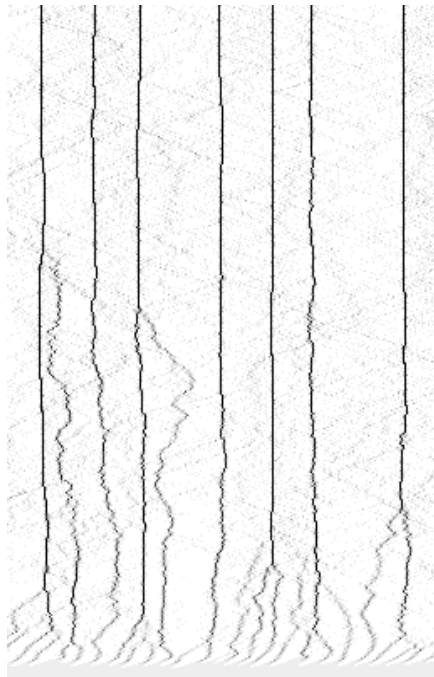


Figure 7. *Localization.* Evolution of the density of energy along the chain. The horizontal axis indicates the position along the chain and the vertical axis corresponds to the time (time is going upward). The grey scale goes from $E_n = 0$ (white) to the maximum E_n (black). Parameters are the same as in figure 6.

This is exactly what we found and what we present in figure 7, where we show the evolution of the density of energy

$$E_n = \frac{1}{2} \dot{u}_n^2 + \frac{1}{4} (u_n - u_{n+1})^2 + \frac{1}{4} (u_{n-1} - u_n)^2 + V(u_n) \quad (25)$$

in grey scales. At the beginning (i.e. at the bottom of the figure), the whole chain is grey which corresponds to an equipartition of the energy through all sites. After a small delay (about 200 periods of the lower edge of the phonons band), the initial linear wave

is completely destroyed because of the modulational instability: the system has reached a state without any coherence. However, we see that some regions are darker than others. These excitations with a small amount of energy are moving as breather-like excitations and interact with others: namely, we find again [3] that the usual property of solitons of passing through each other without energy exchange is destroyed by the discreteness, and moreover, we check that there is a systematic tendency to favour the growth of the larger excitation. The process is, however, regulated by the pinning effect due to the discreteness of the larger excitations [6]: the quasi-stationary final state consists of a few localized modes with most of the energy (the total simulation presented here is about 15 000 periods of the lower-edge phonon band). It is exactly what is called energy localization and, as predicted in a previous article [3], modulational instability is therefore the first step toward energy localization in nonlinear lattices.

If one studies the energy spectrum in the space domain versus time, one sees that, at the end, the spectrum is more or less flat and corresponds to equipartition of energy. Because of the folding of the Brillouin zone, any simple power law scaling k^{-n} failed, in contrast to the case of the Kolmogorov cascade for 3D turbulence (or inverse cascade for 2D turbulence) where an exponent close to $5/3$ is observed over a very substantial range of about three decades of wavenumber [18].

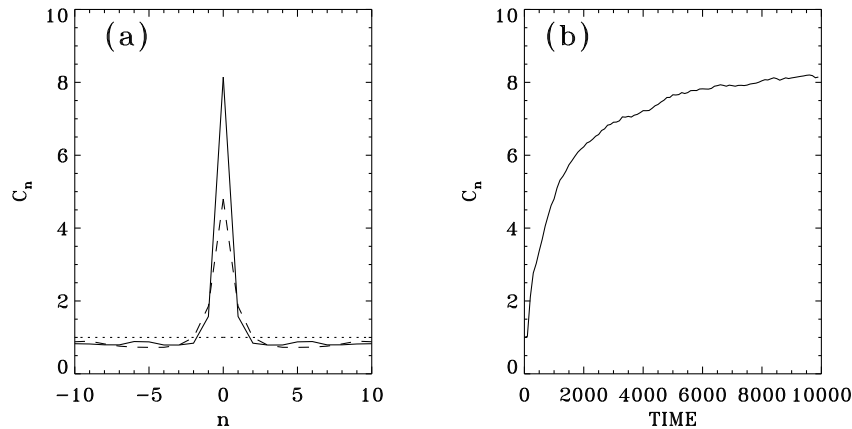


Figure 8. Energy–energy correlation function. (a) C_n for various times; the dotted line corresponds to the initial condition, the dashed line to $t = 1000$ and the solid line to $t = 15000$. (b) Evolution of C_0 versus time (solid line). The parameters are the same as in figure 6.

A more quantitative characterization of the energy localization can be made using the space correlation function

$$C_n(t) = \frac{N \langle \sum_{m=1}^N E_m(t) E_{n+m}(t) \rangle}{\langle \sum_{m=1}^N E_m(t) \rangle^2} \quad (26)$$

where $\langle \cdot \rangle$ indicates an ensemble average. As the initial condition corresponds to a linear wave, $E_n(0)$ is independent of the index n and therefore $C_n(0)$ is equal to 1 for every index n . As shown in figure 7, when time increases the instability destroys the linear wave and therefore a peak develops around $n = 0$ in the energy–energy correlation presented in figure 8(a). This behaviour is explained by the localization of energy since it is not equally distributed on every lattice site. As already suggested [19], this picture also allows us to show that the energy is localized on about five sites and that, even if the amplitude of the

peak is increased, its width is not reduced during the localization process. However, as we show here in figure 8(b), this quantity is maybe even more helpful in measuring the localization of energy versus time and also in emphasizing the saturation effect due to the discreteness.

In summary, we have addressed here the modulational instability as a first step toward energy localization in nonlinear lattices. We have shown that the stability conditions are quantitatively and qualitatively changed by the discreteness. We have also presented a simple explanation of most of the results and finally we were interested in the localization of the energy in discrete lattices. The conclusion is that the energy is localized as breather-like excitations which interact inelastically. This result is important not only to motivate studies on breathers' existence and stability [4, 5], but also for possible physical applications.

References

- [1] Hasegawa A 1985 *Adv. Phys.* **34** 1
- [2] Carnevale G F and Pierrehumbert R T 1992 *Nonlinear Phenomena in Atmospheric and Oceanic Sciences* (New York: Springer)
- [3] Dauxois T and Peyrard M 1993 *Phys. Rev. Lett.* **70** 3995
- [4] Mac Kay R S and Aubry S 1994 *Nonlinearity* **7** 1623
- [5] Flach S 1995 *Phys. Rev. E* **51** 3579
- [6] Dauxois T, Peyrard M and Willis C R 1993 *Phys. Rev. E* **48** 4768
- [7] Benjamin T B and Feir J E 1967 *J. Fluid. Mech.* **27** 417
- [8] Besselov V I and Talanov V I 1966 *Pis'ma Zh. Eksp. Teor. Fiz.* **3** 471 [*JETP Lett.* 1966 **3** 307]
- [9] Tanuiti T and Washimi H 1968 *Phys. Rev. Lett.* **21** 209
- [10] Kivshar Yu S and Peyrard M 1992 *Phys. Rev. A* **46** 3198
- [11] Tsurui A 1972 *Prog. Theor. Phys.* **48** 1196
- [12] Remoissenet M 1986 *Phys. Rev. B* **33** 2386
- [13] A careful derivation (see [14]) of this approximation shows that we obtain the limit of the above expression when $Q \ll 1$ only if $\sin q \tan q \ll \omega^2$, which is not valid close to $q = \pi/2$.
- [14] Daumont I 1994 *Rapport de Magistère* unpublished
- [15] Fermi, Pasta and Ulam 1993 *Los Alamos report: The many body problem* ed D C Mattis (Singapore: World Scientific)
- [16] Yuen H C and Ferguson W E Jr 1978 *Phys. Fluids* **21** 1275
- [17] Zabusky N J and Kruskal M D 1965 *Phys. Rev. Lett.* **15** 240
- [18] Frisch U 1995 *Turbulence* (Cambridge: Cambridge University Press)
- [19] Brown D W, Bernstein L J and Lindenberg K 1996 *Phys. Rev. E* **54** 3352